World Journal of Gastroenterology

Submit a Manuscript: https://www.f6publishing.com

World J Gastroenterol 2025 May 21; 31(19): 104563

DOI: 10.3748/wjg.v31.i19.104563

ISSN 1007-9327 (print) ISSN 2219-2840 (online)

ORIGINAL ARTICLE

Retrospective Study

Development and validation of a radiomics-based prediction model for variceal bleeding in patients with Budd-Chiari syndrome-related gastroesophageal varices

Ze-Dong Wang, Hui-Jie Nan, Su-Xin Li, Lu-Hao Li, Zhao-Chen Liu, Hua-Hu Guo, Lin Li, Sheng-Yan Liu, Hai Li, Yan-Liang Bai, Xiao-Wei Dang

Specialty type: Gastroenterology and hepatology

Provenance and peer review: Unsolicited article; Externally peer reviewed.

Peer-review model: Single blind

Peer-review report's classification

Scientific Quality: Grade A, Grade A, Grade A, Grade A

Novelty: Grade A, Grade A, Grade B, Grade B

Creativity or Innovation: Grade A, Grade A, Grade A, Grade B

Scientific Significance: Grade A, Grade A, Grade A, Grade A

P-Reviewer: Meng QY; Montasser IF

Received: December 28, 2024

Revised: March 24, 2025

Accepted: April 27, 2025

Published online: May 21, 2025

Processing time: 148 Days and 0.7 Hours

Ze-Dong Wang, Su-Xin Li, Lu-Hao Li, Zhao-Chen Liu, Hua-Hu Guo, Lin Li, Sheng-Yan Liu, Xiao-Wei Dang, Department of Hepatopancreatobiliary Surgery, The First Affiliated Hospital of Zhengzhou University, Zhengzhou 450052, Henan Province, China

Ze-Dong Wang, Su-Xin Li, Lu-Hao Li, Zhao-Chen Liu, Hua-Hu Guo, Lin Li, Sheng-Yan Liu, Xiao-Wei Dang, Key Laboratory of Precision Diagnosis and Treatment in General Surgical (Hepatobiliary and Pancreatic) Diseases of Health Commission of Henan Province, The First Affiliated Hospital of Zhengzhou University, Zhengzhou 450052, Henan Province, China

Ze-Dong Wang, Su-Xin Li, Lu-Hao Li, Zhao-Chen Liu, Hua-Hu Guo, Lin Li, Sheng-Yan Liu, Xiao-Wei Dang, Henan Province Engineering Research Center of Minimally Invasive Diagnosis and Treatment of Hepatobiliary and Pancreatic Diseases, The First Affiliated Hospital of Zhengzhou University, Zhengzhou 450052, Henan Province, China

Ze-Dong Wang, Su-Xin Li, Lu-Hao Li, Zhao-Chen Liu, Hua-Hu Guo, Lin Li, Sheng-Yan Liu, Xiao-Wei Dang, Budd-Chiari Syndrome Diagnosis and Treatment Center of Henan Province, The First Affiliated Hospital of Zhengzhou University, Zhengzhou 450052, Henan Province, China

Hui-Jie Nan, Yan-Liang Bai, Department of Hematology, Zhengzhou University People's Hospital and Henan Provincial People's Hospital, Zhengzhou 450003, Henan Province, China

Hai Li, Department of Hepatopancreatobiliary Surgery, Zhengzhou University People's Hospital and Henan Provincial People's Hospital, Zhengzhou 450003, Henan Province, China

Co-first authors: Ze-Dong Wang and Hui-Jie Nan.

Co-corresponding authors: Yan-Liang Bai and Xiao-Wei Dang.

Corresponding author: Xiao-Wei Dang, PhD, Chief Physician, Professor, Department of Hepatopancreatobiliary Surgery, The First Affiliated Hospital of Zhengzhou University, No. 1 Jianshe East Road, Erqi District, Zhengzhou 450052, Henan Province, China.
dangxw1001@zzu.edu.cn

Abstract

BACKGROUND

Budd-Chiari syndrome (BCS) is caused by obstruction of the hepatic veins or suprahepatic inferior vena cava, leading to portal hypertension and the development of gastroesophageal varices (GEVs), which are associated with an increased risk of bleeding. Existing risk models for variceal bleeding in cirrhotic patients have limited applicability to BCS due to differences in pathophysiology. Radiomics, as a noninvasive technique, holds promise as a tool for more accurate prediction of bleeding risk in BCS-related GEVs.

AIM

To develop and validate a personalized risk model for predicting variceal bleeding in BCS patients with GEVs.

METHODS

We retrospectively analyzed clinical data from 444 BCS patients with GEVs in two centers. Radiomic features were extracted from portal venous phase computed tomography (CT) scans. A training cohort of 334 patients was used to develop the model, with 110 patients serving as an external validation cohort. LASSO Cox regression was used to select radiomic features for constructing a radiomics score (Radscore). Univariate and multivariate Cox regression identified independent clinical predictors. A combined radiomics + clinical (R + C) model was developed using stepwise regression. Model performance was assessed using the area under the receiver operating characteristic curve (AUC), calibration plots, and decision curve analysis (DCA), with external validation to evaluate generalizability.

RESULTS

The Radscore comprised four hepatic and six splenic CT features, which predicted the risk of variceal bleeding. Multivariate analysis identified invasive treatment to relieve hepatic venous outflow obstruction, anticoagulant therapy, and hemoglobin levels as independent clinical predictors. The R + C model achieved C-indices of 0.906 (training) and 0.859 (validation), outperforming the radiomics and clinical models alone (AUC: training 0.936 *vs* 0.845 *vs* 0.823; validation 0.876 *vs* 0.712 *vs* 0.713). DCA showed higher clinical net benefit across the thresholds. The model stratified patients into low-, medium- and high-risk groups with significant differences in bleeding rates ($P < 0.001$). An online tool is available at https://bcsvh.shinyapps.io/BCS_Variceal_Bleeding_Risk_Tool/.

CONCLUSION

We developed and validated a novel radiomics-based model that noninvasively and conveniently predicted risk of variceal bleeding in BCS patients with GEVs, aiding early identification and management of high-risk patients.

Key Words: Budd-Chiari syndrome; Gastroesophageal varices; Variceal bleeding; Radiomics; Prognostic model

Core Tip: This study develops a personalized, noninvasive predictive model for variceal bleeding risk in Budd-Chiari syndrome (BCS) patients with gastroesophageal varices. By combining radiomic features from computed tomography imaging with clinical data, the model demonstrated superior predictive performance over traditional approaches, offering a promising tool for early risk assessment and improving patient management in BCS.

Citation: Wang ZD, Nan HJ, Li SX, Li LH, Liu ZC, Guo HH, Li L, Liu SY, Li H, Bai YL, Dang XW. Development and validation of a radiomics-based prediction model for variceal bleeding in patients with Budd-Chiari syndrome-related gastroesophageal varices. *World J Gastroenterol* 2025; 31(19): 104563

URL: https://www.wjgnet.com/1007-9327/full/v31/i19/104563.htm

DOI: https://dx.doi.org/10.3748/wjg.v31.i19.104563

INTRODUCTION

Budd-Chiari syndrome (BCS) is a complex hepatic vascular disorder characterized by the obstruction of the hepatic veins and/or the suprahepatic inferior vena cava, leading to impaired hepatic blood outflow. This obstruction can result in posthepatic portal hypertension, subsequently causing gastroesophageal varices (GEVs)[1-3]. Rupture and bleeding of GEVs are fatal complications associated with high mortality rates linked to portal hypertension. Approximately 50%-60% of patients with liver cirrhosis develop GEVs, with 10%-15% experiencing variceal bleeding annually[4,5]. Therefore, early and accurate prediction of variceal bleeding risk is crucial for timely intervention and improving patient prognosis.

Currently, risk assessment models for variceal bleeding in cirrhotic patients are well established, with endoscopic examination and clinical scoring systems widely utilized. However, the pathophysiological mechanisms of BCS differ from those of cirrhosis, leading to distinct risks and characteristics of GEVs. Existing predictive models have limited applicability in BCS patients[6]. Endoscopy, as an invasive procedure, may cause discomfort and potential complications, especially in patients with severely impaired liver function[7].

Radiomics, an emerging technology, transforms medical imaging into high-dimensional quantitative features, including shape, intensity and texture. This technique can capture complex patterns in imaging data that are difficult for the human eye to discern, providing a more comprehensive risk assessment for portal hypertension and its complications [8-10]. The application of radiomics holds promise for offering more accurate bleeding risk predictions in BCS patients, addressing the limitations of traditional endoscopic evaluations.

The aim of this multicenter study was to develop and validate a radiomics-based predictive model for noninvasive assessment of variceal hemorrhage risk in patients with GEVs associated with BCS, with the aim of providing reliable tools for enhancing clinical decision-making and optimizing patient outcomes.

MATERIALS AND METHODS

Ethical approval and patient selection

This retrospective study was conducted at two tertiary hospitals in Zhengzhou, China: Zhengzhou University First Affiliated Hospital and Zhengzhou University People's Hospital. The study adhered to the ethical principles outlined in the Declaration of Helsinki and was approved by the Ethics Committee of the First Affiliated Hospital of Zhengzhou University (Approval No. 2021-KY-1137-002). As a retrospective observational study, the requirement for informed consent was waived. To ensure confidentiality, all private patient information was deidentified before analysis.

The study included patients diagnosed with BCS complicated by GEVs, with data collected from Zhengzhou University First Affiliated Hospital between January 1, 2016 and December 31, 2021, and Zhengzhou University People's Hospital between January 1, 2016 and December 31, 2022. The diagnosis of BCS was based on criteria from the Chinese Society of Hospital Medicine for Budd-Chiari Syndrome and Liver Vascular Diseases and the European Study Group on Vascular Diseases of the Liver. Imaging modalities such as ultrasound, computed tomography (CT) venography, magnetic resonance venography and digital subtraction angiography were used to confirm the presence of vascular outflow obstruction. Enhanced CT imaging was utilized by two experienced radiologists to confirm the diagnosis of GEVs and generate imaging reports.

Participants were included if they met the following criteria: (1) Definitive diagnosis of BCS based on imaging evidence of venous outflow obstruction; and (2) First-time diagnosis of GEVs based on three-phase enhanced CT imaging. Patients were excluded if they met any of the following criteria: (1) Previous variceal treatment; (2) Presence of malignant tumors; (3) Other liver diseases such as viral, alcoholic or autoimmune hepatitis; (4) Incomplete or poor-quality imaging or clinical data; (5) In-hospital death or concurrent severe organ dysfunction; (6) Transjugular intrahepatic portosystemic shunt (TIPS) for massive ascites; or (7) Prophylactic treatment for GEVs during follow-up. The inclusion and exclusion process is summarized in Figure 1.

Image preprocessing and feature extraction

Each patient underwent a standardized GE 64-row spiral CT examination. Patients were instructed to fast for 6-8 hours before scanning, and an iodine allergy test was conducted. For patients without iodine allergy, 800-1000 mL of warm water was consumed 5 minutes before scanning to ensure adequate gastric filling. Scanning parameters included a tube voltage of 120 kVp, tube current of 290-650 mA and scan thickness of 5.0 mm. Contrast-enhanced scans were performed using iodixanol (300 mgI/mL) as the contrast agent, with a weight-adjusted dose administered at 2.5-3.5 mL/s. Images were acquired during the arterial (approximately 30 seconds postinjection) and venous (60-70 seconds postinjection) phases and reconstructed on the AW4.4 workstation with a slice thickness of 0.63 mm.

To avoid any variations in scanning accuracy and three-dimensional (3D) reconstruction between centers, all imaging examinations at both hospitals were performed using identical GE 64-row spiral CT scanners, strictly standardized acquisition protocols and the same 3D reconstruction software. This uniformity ensures that any potential differences attributable to device or software variability are effectively minimized, thereby providing consistent imaging data processing and reliable radiomics feature extraction.

Two regions of interest (ROIs) were manually delineated at the hepatic (Figure 2A) and splenic (Figure 2B) hilum levels using 3D Slicer (version 5.6.1). Two experienced radiologists (each with > 7 years of experience) independently segmented the ROIs, ensuring that they captured relevant anatomical structures while excluding major blood vessels, artefacts, and focal hepatic lesions. Any inconsistencies were resolved through discussion with a senior radiologist (> 15 years of experience). To validate segmentation consistency, the ROIs were independently redrawn by two experienced radiologists (Reader 1 and Reader 2), and the intraclass correlation coefficient (ICC) values above 0.75 confirmed high reproducibility.

Radiomic features were extracted from the delineated ROIs using PyRadiomics (version 3.1.0). Preprocessing steps included Z-score normalization to standardize feature distributions, grayscale discretization into 25 bins, and symmetrical gray-level co-occurrence matrix (GLCM) enforcement to improve texture feature reproducibility. Voxel resampling was not applied due to consistent voxel spacing across datasets. A total of 851 radiomic features were extracted for each ROI, spanning seven categories: shape (14), first-order intensity (162), and second-order texture features, including gray-level co-occurrence matrix (216), gray-level run length matrix (144), gray-level size zone matrix

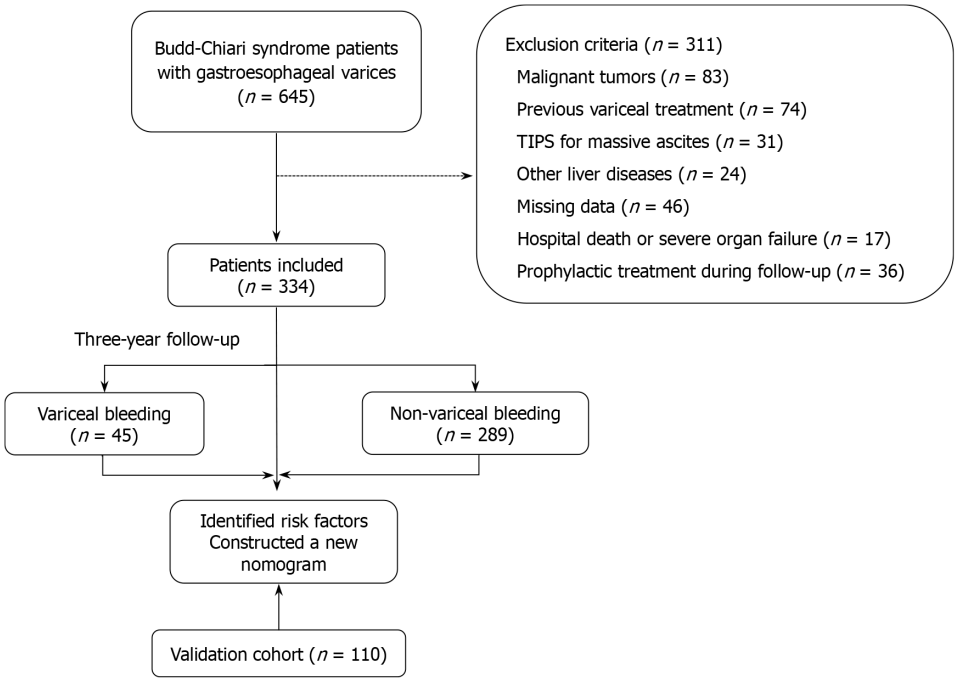

Figure 1 Study flow chart. TIPS: Transjugular intrahepatic portosystemic shunt.

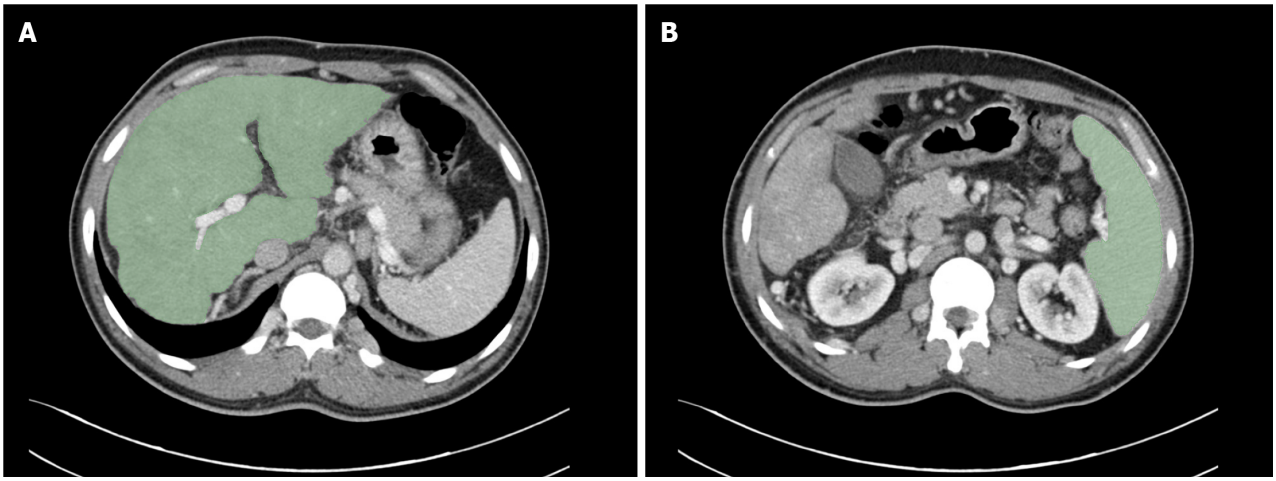

Figure 2 Regions of interest for the liver and spleen. A: Region of interest (ROI) for the liver delineated at the hepatic hilum; B: ROI for the spleen delineated at the splenic hilum.

(144), gray-level dependence matrix (126), and neighbouring gray tone difference matrix (45). In total, 1702 features (851 per ROI) were extracted for subsequent analysis.

Clinical and radiomics data

The clinical data included key demographic, laboratory and imaging parameters relevant to bleeding risk and BCS severity. Imaging parameters derived from contrast-enhanced CT scans included measurements reflecting vascular obstruction and splenic and portal hemodynamics. These parameters were selected based on their clinical relevance and ease of measurement, ensuring consistency and reproducibility across retrospective datasets.

Extracted radiomic features underwent preprocessing to ensure consistency and comparability across datasets. Features were standardized using *Z*-score normalization, and feature selection was performed to identify the most predictive radiomic variables for model development. The selected features were integrated with clinical data to develop predictive models for bleeding risk.

Follow-up and outcomes

The follow-up period was set at 3 years (or until the occurrence of a bleeding event, whichever occurred first). The primary endpoint of the study was the initial occurrence of esophagogastric variceal bleeding, which was confirmed through clinical diagnosis. This diagnosis was based on pertinent clinical manifestations of upper gastrointestinal

bleeding, such as hematemesis and/or melena, that necessitated treatment *via* endoscopic therapy, interventional procedures, or surgery. Patients with upper gastrointestinal bleeding caused by ulcers, gastric diseases related to portal hypertension, or other nonvariceal factors were excluded.

Statistical analysis

The statistical analysis was conducted using SPSS 26, R 4.2.3, and X-tile. Normally distributed quantitative data are presented as mean ± SD, and group comparisons were performed using *t* tests, while non-normally distributed data were expressed as M (Q1, Q3) and compared using Mann-Whitney *U* tests. Numerical data were reported as frequencies (percentages) and analyzed using χ^2 tests or Fisher's exact test. Independent risk factors for bleeding were identified through univariate and multivariate Cox regression analyses. LASSO Cox regression was applied for radiomic feature selection, thereby reducing the dimensionality of the data. The penalty parameter (λ) was optimized *via* 10-fold cross-validation based on the minimum deviance criterion. The proportional hazards assumption was validated using a multivariate Cox model. The receiver operating characteristic (ROC) curve for the predictive model was visualized using the rms package and deployed as a web tool on shinyapp.io *via* DynNom. Model discrimination was evaluated using the C index and its 95% confidence interval (95%CI), while calibration was assessed using a calibration curve generated with the rms package. Clinical efficacy was evaluated through decision curve analysis (DCA) using the ggDCA package. The optimal risk score cut-off for hierarchical risk classification was determined using X-tile. Kaplan-Meier survival analysis was performed, with significance set at $P < 0.05$.

RESULTS

Patient demographics and baseline characteristics (bleeding vs nonbleeding groups)

A total of 444 BCS patients with GEVs were included in this study. The mean age of the cohort was 51.5 ± 10.9 years (range 21-85 years), and 58.9% were male. During the follow-up period, 61 patients (13.7%) experienced their first variceal bleeding event. Patients were classified into the bleeding group (n = 61) and the nonbleeding group (n = 383). A comparison of baseline characteristics between the two groups is presented in Table 1.

Patients in the bleeding group had significantly lower platelet counts, albumin levels and sodium levels but higher creatinine, aspartate aminotransferase (AST), Child-Pugh grade, albumin-bilirubin score, and Model for End-stage Liver Disease score (all $P < 0.05$). In contrast, fewer patients in the bleeding group had undergone invasive treatment to relieve hepatic venous outflow obstruction compared to the nonbleeding group ($P < 0.001$), suggesting a potential protective effect of this intervention (Table 1).

Comparison of the training and validation cohorts

To develop and validate the risk prediction model, patients from the First Affiliated Hospital of Zhengzhou University (n = 334) were designated as the training cohort, whereas those from Zhengzhou University People's Hospital (n = 110) constituted the validation cohort. There were no significant differences (all $P > 0.05$) in baseline demographics, clinical parameters or imaging findings between these two cohorts (Table 2). Such comparability ensures a robust basis for subsequent model development and external validation.

Radiomics feature selection and clinical correlation analysis

A total of 1702 radiomic features were extracted per patient, with 851 features from each ROI. To ensure data stability, reliability was assessed by computing the ICC for a randomly selected subset of 30 patients. Features with ICC > 0.75 were retained, resulting in 1333 reliable radiomic features for subsequent analysis. Feature selection was performed using LASSO Cox regression with 10-fold cross-validation to optimize the penalty parameter (λ), which identified 10 nonzero radiomic features for constructing the Radscore (Figure 3). These features included nine wavelet-transformed texture features and one GLCM-derived feature, reflecting their relevance in capturing multi-scale texture patterns and texture coarseness (Supplementary Table 1). Univariate Cox regression analysis of clinical variables revealed significant associations with sex, portal vein thrombosis, invasive treatment to relieve hepatic venous outflow obstruction, use of anticoagulant medication, ascites, spleen thickness, red blood cell count, hemoglobin level, platelet count, serum sodium level, creatinine level, AST level, alkaline phosphatase level, albumin level, direct bilirubin level, prothrombin time, BCS type, and Child-Turcotte-Pugh class. Multivariate Cox regression further identified three independent risk factors for GEV bleeding in BCS patients. Invasive treatment to relieve hepatic venous outflow obstruction, use of anticoagulant medication and hemoglobin levels (Table 3). These variables were used to construct a clinical-only risk prediction model (C model), which demonstrated significant predictive performance.

Development and validation of a prognostic model for GEV bleeding

To construct a comprehensive risk prediction model, the radiomics-based Radscore was integrated with significant clinical variables identified through multivariate Cox regression analysis. The final model revealed that the following were independent risk factors for bleeding in patients with BCS. Invasive treatment to relieve hepatic venous outflow obstruction [hazard ratio (HR) = 0.089, 95%CI = 0.044-0.181, $P < 0.001$), use of anticoagulants (HR = 10.653, 95%CI = 3.102-36.582, $P < 0.001$), gender (HR = 2.332, 95%CI = 1.057-5.144, $P = 0.036$), platelet count (HR = 0.992, 95%CI = 0.984-0.999, $P = 0.035$), and Radscore (HR = 1.545, 95%CI = 1.236-1.932, $P < 0.001$). These variables were incorporated into a nomogram for individualized prediction (Figure 4). The predictive accuracy of the radiomics + clinical (R + C) model was assessed

Table 1 Baseline characteristics of Budd-Chiari syndrome patients with gastroesophageal varices stratified by variceal bleeding status

Variables	Bleeding group (*n* = 61)	Non-bleeding group (*n* = 383)	*P* value
Age (years)	52.1 ± 11.2	51.4 ± 10.8	0.640
Sex (male)	50 (82)	209 (54.6)	< 0.001
Diabetes	3 (4.9)	29 (7.6)	0.633
Ascites	33 (54.1)	144 (37.6)	0.015
Hepatic encephalopathy	2 (3.3)	11(2.9)	1.000
IVC or HV thrombosis	9 (14.8)	79 (20.6)	0.285
Portal vein thrombosis	7 (11.5)	16 (4.2)	0.038
Spleen thickness (mm)	46 (39, 58)	45 (39, 49)	0.041
Portal vein diameter (mm)	12.7 (10.0, 14.5)	12.7 (10.0, 15.0)	0.994
BCS type			0.042
HV type	19 (31.1)	67 (17.5)	
Mixed type	35 (57.4)	269 (70.2)	
IVC type	7 (11.5)	47 (12.3)	
Child-Pugh grade			< 0.001
A	26 (42.6)	256 (66.8)	
B	21 (34.4)	121 (31.6)	
C	14 (23)	6 (1.6)	
ALBI, median (IQR)	-2.07 (-2.57, -1.28)	-2.38 (-2.75, -1.97)	< 0.001
MELD, median (IQR)	8.22 (4.07, 13.00)	4.15 (1.72, 7.19)	< 0.001
Use of anticoagulant medication	56 (91.8)	310 (80.9)	0.038
Invasive treatment to relieve hepatic venous outflow obstruction	27 (44.3)	344 (89.8)	< 0.001
White blood cell (× 10^9/L)	3.8 (2.9, 5.0)	3.4 (2.7, 4.5)	0.271
Red blood cell (× 10^{12}/L)	3.7 (2.8, 4.4)	4.0 (3.6, 4.4)	0.016
Hemoglobin (g/L)	115 (77.5, 134.0)	124 (109, 138)	0.005
Platelet (× 10^9/L)	71 (48.5, 98)	90 (67, 126)	< 0.001
Sodium (mmol/L)	140 (137.5, 142.0)	142 (140, 143.9)	< 0.001
Creatinine (μmol/L)	62 (48.5, 76.5)	55 (46, 65)	0.007
Alanine aminotransferase (U/L)	23 (19, 39.5)	21 (17, 27)	0.019
Aspartate aminotransferase (U/L)	32 (23.5, 50)	27 (23, 34)	0.001
Gamma-glutamyl transferase (U/L)	74 (41, 151)	60.6 (36.5, 111)	0.065
Alkaline phosphatase (U/L)	106 (80.6, 142)	90 (72, 117)	0.006
Total protein (g/L)	61.1 (54.1, 66.9)	63.2 (58.7, 67.8)	0.018
Albumin (g/L)	33.2 (28.7, 39.8)	38.3 (34, 42)	< 0.001
Total bilirubin (μmol/L)	26.5 (14.8, 60.2)	21 (14.1, 31.5)	0.015
Prothrombin time (s)	16.3 (14.7, 18.5)	14.6 (13.7, 16.0)	< 0.001

BCS: Budd-Chiari syndrome; IVC: Inferior vena cava; HV: Hepatic veins; ALBI: Albumin-bilirubin; MELD: Model for end-stage liver disease.

using the C-index, which achieved values of 0.906 in the training set and 0.859 in the validation set, indicating excellent discrimination. The R + C model demonstrated better predictive performance compared to the clinical-only model (C model) and the radiomics-only model (Radscore; Table 4). ROC curves were generated to assess model discrimination over a 3-year follow-up period. The results showed that the R + C model achieved superior discrimination compared to the individual Radscore and C model, as reflected by its larger AUC in both the training and validation datasets (Figure 5). Calibration curves confirmed a strong alignment between predicted and observed outcomes (Figure 6), while

Table 2 Comparison of patient characteristics between the training and validation cohorts

Variables	Training cohort (*n* = 334)	Validation cohort (*n* = 110)	*P* value
Age (years)	51.4 ± 11.1	51.9 ± 10.3	0.663
Sex (male)	193 (57.8)	66 (60)	0.683
Diabetes	26 (7.8)	6 (5.5)	0.412
Ascites	131 (39.2)	46 (41.8)	0.630
Hepatic encephalopathy	10 (3)	3 (2.7)	1
IVC or HV thrombosis	60 (18)	28 (25.5)	0.087
Portal vein thrombosis	20 (6)	3 (2.7)	0.181
Spleen thickness (mm)	45 (39, 49)	43 (38, 51)	0.700
Portal vein diameter (mm)	12.7 (10.2, 14.6)	12.7 (10, 15)	0.763
BCS type			0.389
HV type	69 (20.6)	17 (15.5)	
Mixed type	227 (68)	77 (70)	
IVC type	38 (11.4)	16 (14.5)	
Child-Pugh grade			0.683
A	210 (62.9)	72 (65.4)	
B	110 (32.9)	32 (29.1)	
C	14 (4.2)	6 (5.5)	
ALBI, median (IQR)	-2.34 (-2.74, -1.89)	-2.31 (-2.64, -1.85)	0.494
MELD, median (IQR)	4.74 (2.18, 8.00)	4.14 (1.60, 7.34)	0.252
Use of anticoagulant medication	271 (81.1)	73 (66.4)	0.001
Invasive treatment to relieve hepatic venous outflow obstruction	276 (82.6)	95 (86.4)	0.360
White blood cell (× 10^9/L)	3.4 (2.7, 4.4)	3.7 (2.7, 5.0)	0.107
Red blood cell (× 10^{12}/L)	4.0 (3.5, 4.4)	4 (3.6, 4.6)	0.145
Hemoglobin (g/L)	122 (105, 136)	124 (106, 140.3)	0.358
Platelet (× 10^9/L)	86 (65, 118.3)	91 (67, 141)	0.434
Sodium (mmol/L)	142 (140, 143.5)	142 (140, 143.3)	0.677
Creatinine (μmol/L)	56 (47, 67)	55 (44, 65.3)	0.251
Alanine aminotransferase (U/L)	22 (17, 27.2)	19.7 (15.6, 29.1)	0.126
Aspartate aminotransferase (U/L)	28 (23, 35)	27.3 (21.7, 34.5)	0.357
Gamma-glutamyl transferase (U/L)	61 (35.8, 117)	64.2 (45.0, 111.6)	0.272
Alkaline phosphatase (U/L)	92 (72, 121.3)	96.4 (79, 127.3)	0.273
Total protein (g/L)	63.2 (58.5, 67.7)	62.6 (57.6, 67.6)	0.526
Albumin (g/L)	38 (33.3, 41.8)	37.7 (33.3, 41.3)	0.672
Total bilirubin (μmol/L)	21 (13.9, 33.4)	22.8 (15.1, 35.4)	0.536
Prothrombin time (s)	14.8 (13.8, 16.4)	14.6 (13.2, 16.1)	0.064

BCS: Budd-Chiari syndrome; IVC: Inferior vena cava; HV: Hepatic veins; ALBI: Albumin-bilirubin; MELD: Model for end-stage liver disease.

DCA demonstrated the superior net clinical benefit of the R + C model across a wide range of threshold probabilities (Figure 7).

Clinical performance and risk stratification

According to the R + C model, the risk analysis was performed for individuals diagnosed with BCS complicated by GEVs. The relevant equation was as follows: Risk assessment = 0.847 Sex - 0.008 platelet count - 2.417 invasive treatment to

Table 3 Univariate and multivariate analyses of factors associated with gastroesophageal variceal bleeding in patients with Budd-Chiari syndrome and gastroesophageal varices

Variables	Univariate cox regression		Multivariate cox regression	
	HR (95%CI)	*P* value	HR (95%CI)	*P* value
Age	0.994 (0.968-1.020)	0.646		
Sex	3.621 (1.686-7.777)	0.001		
Hepatic encephalopathy	0.712 (0.098-5.166)	0.737		
Diabetes	0.535 (0.130-2.209)	0.388		
Portal vein thrombosis	3.329 (1.486-7.460)	0.003		
IVC or HV thrombosis	0.696 (0.295-1.645)	0.409		
Invasive treatment to relieve hepatic venous outflow obstruction	0.127 (0.070-0.230)	< 0.001	0.123 (0.048-0.318)	<0.001
Use of anticoagulant medication	3.408 (1.056-10.994)	0.040	8.905 (2.296-34.534)	0.002
Ascites	1.798 (1.001-3.229)	0.050		
Portal vein diameter (mm)	1.003 (0.915-1.099)	0.953		
Spleen thickness (mm)	1.041 (1.015-1.068)	0.002		
White blood cell ($\times 10^9$/L)	1.071 (0.946-1.221)	0.271		
Red blood cell ($\times 10^{12}$/L)	0.563 (0.388-0.818)	0.003		
Hemoglobin (g/L)	0.976 (0.965-0.986)	< 0.001	0.974 (0.955-0.994)	0.012
Platelet ($\times 10^9$/L)	0.988 (0.979-0.997)	0.006		
Sodium (mmol/L)	0.828 (0.773-0.887)	< 0.001		
Creatinine (μmol/L)	1.025 (1.014-1.037)	< 0.001		
Aspartate aminotransferase (U/L)	1.009 (1.001-1.017)	0.020		
Gamma-glutamyl transferase (U/L)	1.000 (0.998-1.002)	0.864		
Alkaline phosphatase (U/L)	1.004 (1.002-1.007)	0.002		
Albumin	0.899 (0.861-0.939)	< 0.001		
Direct bilirubin	1.012 (1.007-1.016)	< 0.001		
Prothrombin time	1.080 (1.047-1.113)	< 0.001		
BCS type		0.081		
Mixed type *vs* HV type	0.501 (0.265-0.945)	0.033		
IVC type *vs* HV type	0.450 (0.149-1.355)	0.156		
Child		< 0.001		
B *vs* A	1.408 (0.706-2.808)	0.311		
C *vs* A	14.353 (6.881-29.937)	< 0.001		

HR: Hazard ratio; 95%CI: 95% confidence interval; BCS: Budd-Chiari syndrome; IVC: Inferior vena cava; HV: Hepatic veins; ALBI: Albumin-bilirubin; MELD: Model for end-stage liver disease.

relieve hepatic venous outflow obstruction + 2.366 use of anticoagulant medication + 0.435 Radscore. The specific threshold was identified through X-tile, and all participants were classified into low-, moderate- or high-risk categories according to their likelihood of bleeding (low risk: < 0.57; medium risk: 0.57-1.11; high risk: > 1.11). In the training set, the cumulative occurrence rates of variceal hemorrhage were 2.2%, 14.7% and 85.3% for the low-, moderate- and high-risk groups, respectively (log-rank test, $P < 0.001$; Figure 8A). Within the validation group, the cumulative incidence rates were 3.9%, 17.4% and 90% for each group (log-rank test, $P < 0.001$; Figure 8B), which suggests that the model effectively differentiated the risk of variceal bleeding in patients with BCS complicated by GEVs.

Table 4 C-indices of various models

Variables	Training cohort			Validation cohort		
	C-index (95%CI)	AIC	*P* value	C-index (95%CI)	AIC	*P* value
R + C model	0.906 (0.864-0.947)	407.267	-	0.859 (0.761-0.958)	112.684	-
R model	0.825 (0.761-0.889)	474.138	0.006	0.706 (0.566-0.846)	142.004	0.015
C model	0.802 (0.724-0.879)	442.580	0.003	0.699 (0.539-0.859)	136.163	0.035
MELD	0.721 (0.646-0.796)	481.666	< 0.001	0.635 (0.485-0.786)	147.129	0.002
ALBI	0.667 (0.581-0.753)	490.816	< 0.001	0.634 (0.491-0.776)	147.705	0.004

R + C: Radiomic + clinical model; R: Radiomic model; C: Clinical model; MELD: Model for end-stage liver disease; ALBI: Albumin-bilirubin; 95%CI: 95% confidence Interval; AIC: Akaike information criterion.

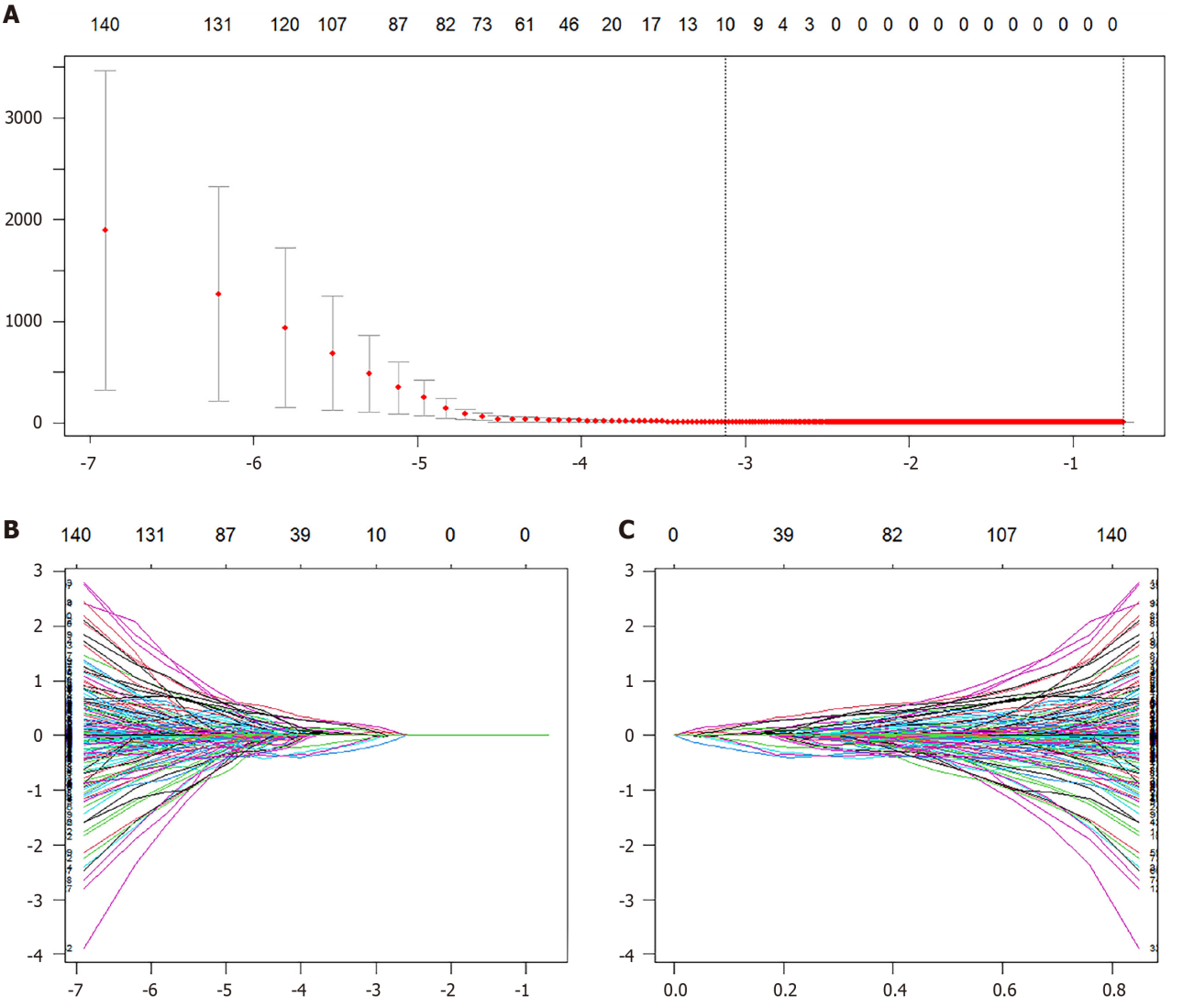

Figure 3 The LASSO-regularized Cox regression for radiomics feature selection is illustrated. Ten-fold cross-validation was used to determine the optimal model parameter (*λ*). A: Relationship between the partial likelihood deviance and log(*λ*), which aided in selecting the optimal *λ* value; B: Coefficient profiles of all candidate features as a function of log(*λ*), with each colored line representing a different feature; C: Trajectories of the feature coefficients relative to the fraction of deviance explained.

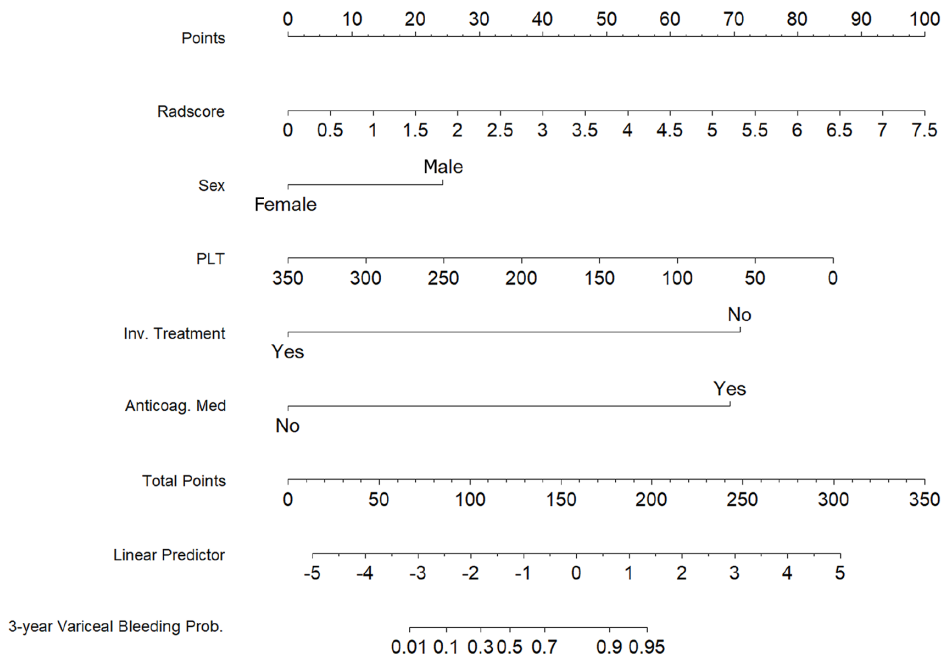

Figure 4 Nomogram for predicting the probability of variceal hemorrhage in patients with gastroesophageal varices associated with Budd-Chiari syndrome. PLT: Platelet count; Inv.Treatment: Invasive treatment to relieve hepatic venous outflow obstruction; Anticoag.med: Use of anticoagulant medication.

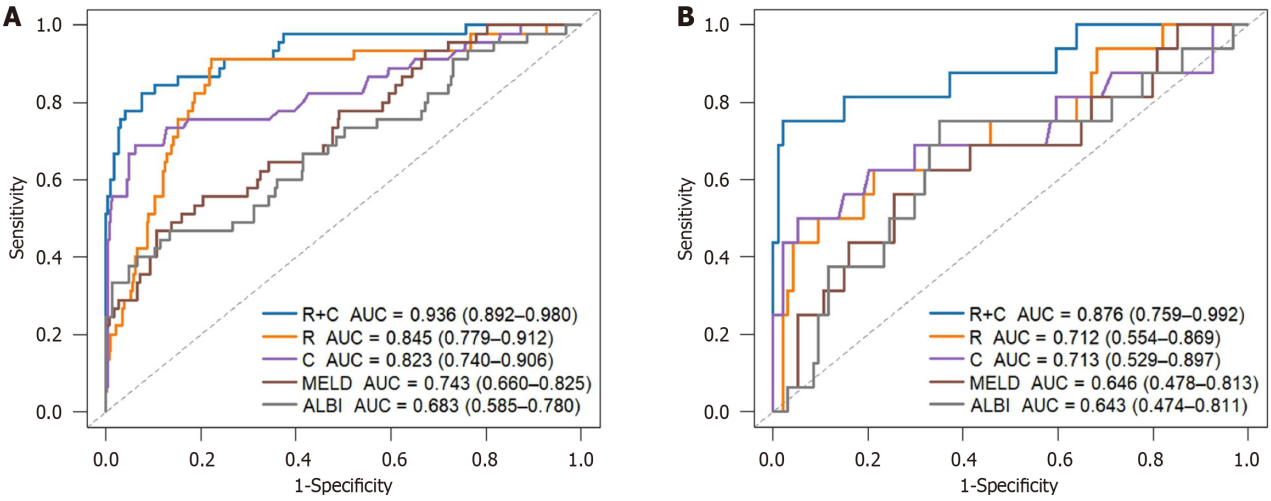

Figure 5 Receiver operating characteristic curves of the nomogram. A: Receiver operating characteristic (ROC) curve in the training cohort; B: ROC curve in the validation cohort. R + C: Radiomic + clinical model; R: Radiomic model; C: Clinical model; MELD: Model for end-stage liver disease; ALBI: Albumin-bilirubin; AUC: The area under the receiver operating characteristic curves.

DISCUSSION

This study successfully developed and validated a noninvasive risk prediction model (R + C model) by integrating radiomics features with clinical characteristics to evaluate the risk of first variceal bleeding in BCS patients with GEVs. The model incorporated Radscore and key clinical predictors, such as invasive treatments to alleviate hepatic venous outflow obstruction, anticoagulation use, sex, and platelet count, significantly enhancing the accuracy of bleeding risk prediction. This model provides an effective tool for the management and treatment of BCS patients.

Radiomics technology, as a novel imaging analysis method, has been extensively applied in the oncology field[11-14]. It has also shown substantial potential in diagnosing and predicting outcomes in non-oncological liver diseases, such as liver fibrosis and portal hypertension syndrome[4,15-18]. For example, Luo *et al*[15] successfully predicted the risk of bleeding in cirrhotic patients by constructing liver and spleen radiomics models. Zhang *et al*[4] explored the risk of variceal bleeding in hepatitis-B-related cirrhotic patients within 1 year. Due to the distinct pathophysiological characteristics of BCS, which mainly manifest as hepatic venous outflow obstruction, the risk of variceal bleeding and treatment response in BCS patients differ significantly from those in cirrhotic patients[19,20]. China, being the country with the

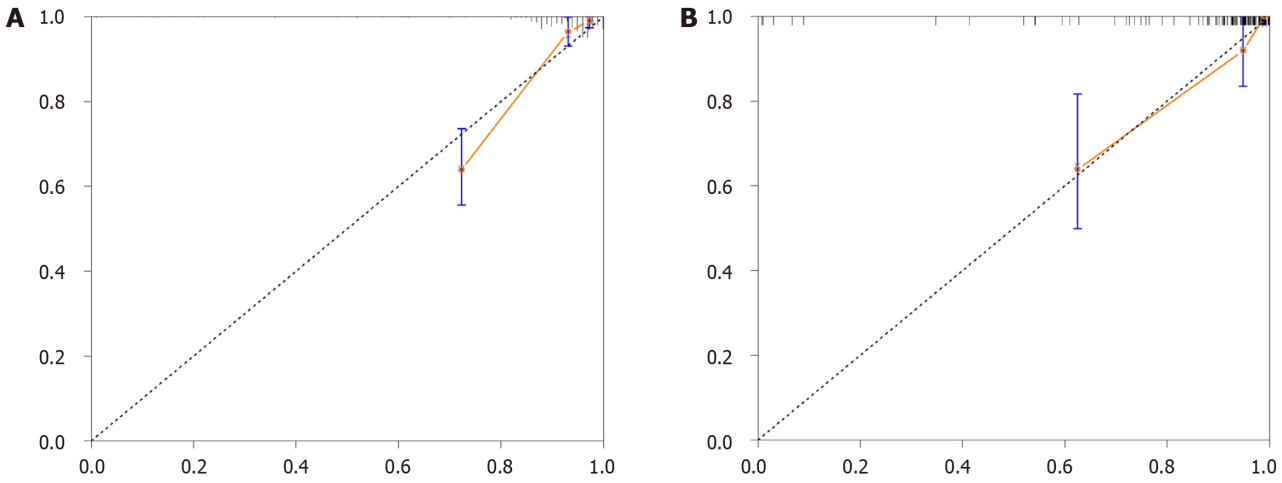

Figure 6 Calibration curves of the radiomic and clinical model. A: Calibration curve in the training cohort; B: Calibration curve in the validation cohort.

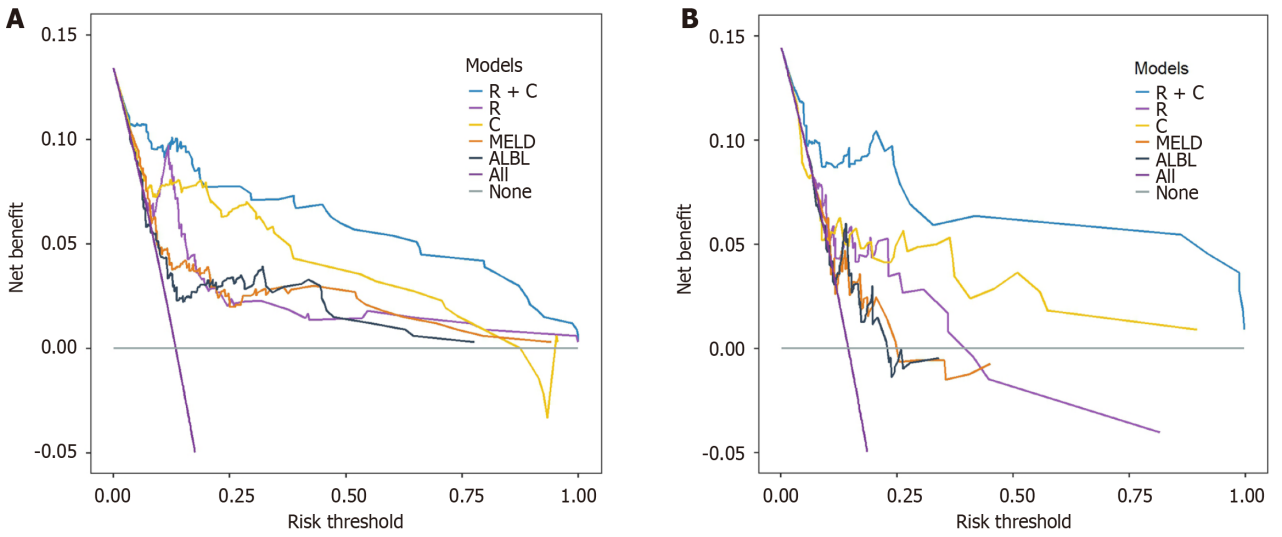

Figure 7 Decision curve analysis of the nomogram. A: Decision curve analysis (DCA) in the training cohort; B: DCA in the validation cohort. R + C: Radiomic + clinical model; R: Radiomic model; C: Clinical model; MELD: Model for end-stage liver disease; ALBI: Albumin-bilirubin.

highest number of diagnosed BCS cases globally, still lacks a comprehensive risk prediction model for variceal bleeding in BCS patients[21,22]. This study innovatively combined liver and spleen radiomics features with clinical factors, significantly improving the predictive ability for variceal bleeding risk in BCS patients. It enables the development of more precise treatment strategies based on individual risk levels, thereby optimizing personalized management and significantly improving patient outcomes.

In this study, we found that invasive treatments and anticoagulation therapy are independent risk factors for variceal bleeding in BCS patients with GEVs. Invasive treatments, such as TIPS and angioplasty, effectively reduce the risk of variceal bleeding by relieving hepatic venous outflow obstruction and lowering portal pressure[3]. However, invasive procedures themselves carry a risk of treatment-related bleeding events (*e.g.*, procedural site bleeding or abdominal hemorrhage), which are typically observed within 24-48 hours post-procedure. Although this type of bleeding is distinct from variceal bleeding, as it is more closely associated with procedural trauma and the intensity of pre-procedural anticoagulation therapy, it highlights the complex interplay between invasive treatments and anticoagulation management in BCS patients. For example, Rautou *et al*[23] reported that in BCS patients undergoing TIPS or other invasive treatments, excessive pre-procedural anticoagulation significantly increased the risk of procedural bleeding events, underscoring the need for balanced anticoagulation protocols. Similarly, our study identified anticoagulation therapy as an independent risk factor for variceal bleeding, which may reflect the broader challenge of managing anticoagulation intensity and timing in BCS patients with GEVs. These findings emphasize the importance of tailoring anticoagulation therapy to individual patient needs, especially in the context of invasive treatments, to minimize both treatment-related and variceal bleeding risks.

Although invasive treatments are beneficial in reducing portal pressure and the long-term risk of variceal bleeding, inappropriate anticoagulation therapy [*e.g.*, excessive dosage, improper timing, or insufficient international normalized ratio (INR) monitoring] may exacerbate the risk of variceal bleeding[24]. In BCS patients with GEVs, this risk may be

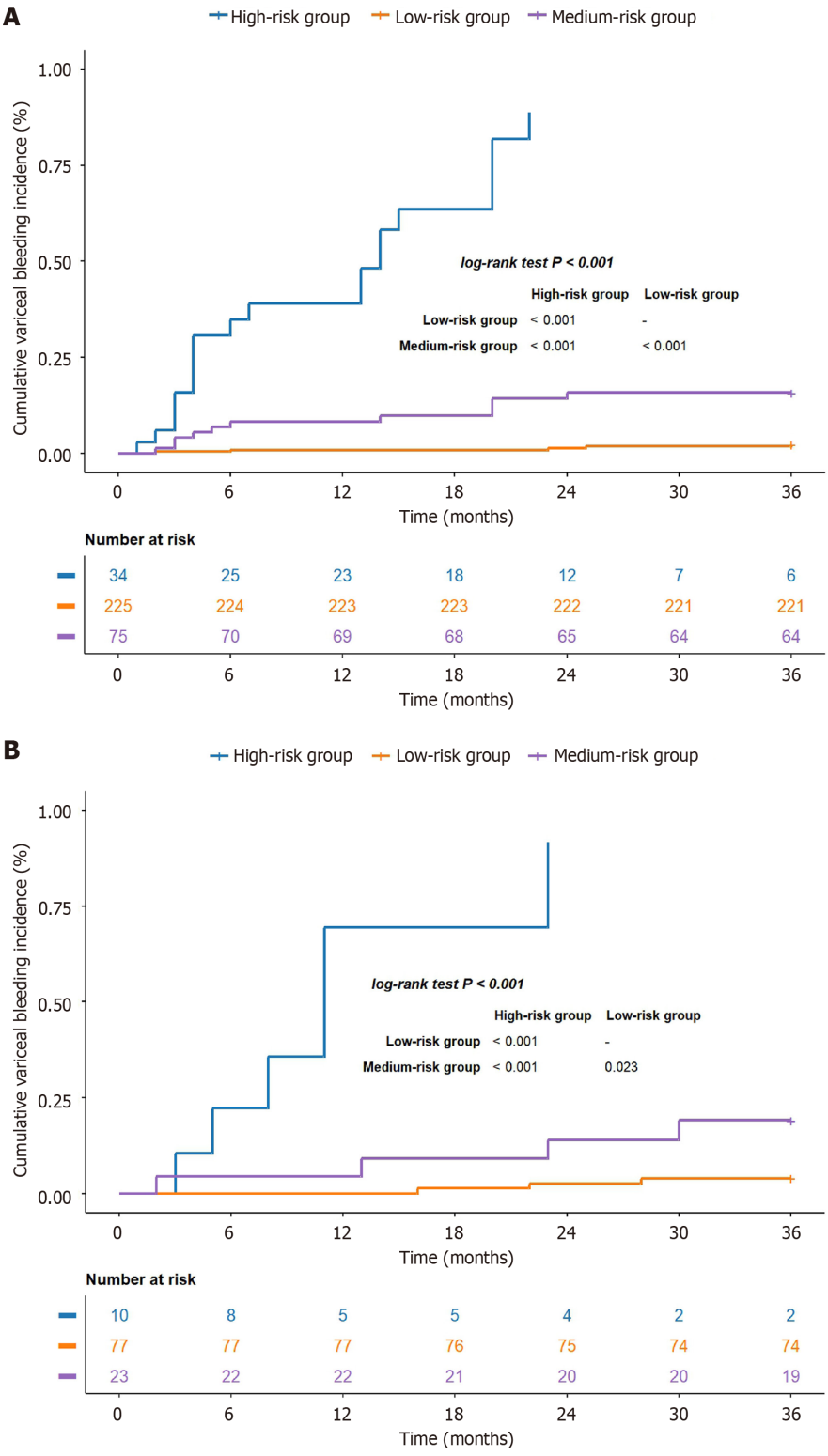

Figure 8 Cumulative risk curves stratified by the risk score. A: Cumulative risk curve in the training cohort; B: Cumulative risk curve in the validation cohort.

further amplified due to existing portal hypertension and variceal fragility. Our findings suggest that careful evaluation and optimization of anticoagulation protocols are critical for balancing the risks and benefits of therapy. Specifically, for patients undergoing invasive treatments, it is necessary to comprehensively evaluate the intensity and timing of anticoagulation therapy before, during and after the procedure. Strict adherence to anticoagulation protocols, including individualized dosing and careful INR monitoring, can mitigate the risk of variceal bleeding while preventing treatment-related bleeding events. Additionally, future research should focus on developing evidence-based guidelines to further refine anticoagulation management strategies in BCS patients.

Our study identified male sex as a significant risk factor for variceal bleeding, in contrast to previous studies that reported a higher incidence of portal-hypertension-related complications in female patients[25,26]. This discrepancy may be attributed to differences in patient characteristics, study design or clinical management strategies. In our cohort, male patients demonstrated a higher mean spleen thickness (46.36 mm *vs* 42.99 mm) and portal vein diameter (12.98 mm *vs* 12.00 mm) compared to females; both of which are recognized markers of severe portal hypertension. These findings may indirectly contribute to the observed increased bleeding risk in male patients. Additionally, it is possible that male patients were less adherent to anticoagulation protocols or presented with more advanced disease at the time of diagnosis, as suggested by prior studies in similar populations[27]. Hormonal differences, such as the vascular protective effects of estrogen in females, might also play a role in reducing bleeding risk in female patients. However, these hypotheses could not be directly evaluated in the present study due to the retrospective design and require further investigation in larger, prospective cohorts. Understanding these sex-based variations is essential for tailoring individualized management strategies in BCS patients with GEVs.

Platelet count also plays a crucial role in assessing bleeding risk. BCS patients often develop splenomegaly, resulting in thrombocytopenia, which indicates increased portal hypertension severity and a higher risk of variceal bleeding[28,29]. Our findings confirmed that low platelet count is significantly associated with bleeding risk, thereby improving the model's predictive capability and offering clinicians a more comprehensive assessment tool.

In terms of diagnostic methods, this study used portal venous phase contrast-enhanced CT, which not only facilitates the diagnosis of BCS but also effectively evaluates GEVs, providing a comprehensive assessment of patients[30,31]. Compared with traditional endoscopy, enhanced CT offers noninvasive, highly sensitive and simultaneous evaluation of hepatic and splenic hemodynamics[32-34]. This imaging technology serves as a reliable alternative for patients unsuitable for endoscopy, reducing discomfort and potential complications during examinations and providing crucial pathophysiological information for clinical decision-making.

The risk stratification system based on the R + C model divided patients into low-, medium-, and high-risk groups, with a significant difference in variceal bleeding incidence between the groups. The bleeding incidence in the high-risk group was significantly higher than that in the medium- and low-risk groups. This risk stratification system offers valuable guidance for the clinical management of BCS patients with GEVs.

In this study, the bleeding rate in the high-risk group reached 85.3%, indicating a high risk of variceal rupture and bleeding. For these patients, we recommend active preventive interventions, such as endoscopic treatment (*e.g.*, endoscopic variceal ligation or sclerotherapy)[35]. Additionally, if high-risk patients experience recurrent hepatic venous outflow obstruction or other portal-hypertension-related complications (*e.g.*, symptoms of portal hypertension not effectively controlled by medication or endoscopic therapy), TIPS treatment should be considered under certain circumstances even if the standard indications for TIPS have not yet been met[36]. TIPS can improve hepatic venous outflow and reduce portal pressure, thereby decreasing the risk of variceal bleeding. It is a safe and effective treatment option[37]. Therefore, for high-risk patients, a comprehensive assessment of their condition and potential benefits should be conducted, and TIPS intervention should be actively considered when necessary to prevent bleeding events.

For medium-risk patients, the bleeding rate was 14.7%, comparable to the annual bleeding rate reported in cirrhotic patients with GEVs (10%-15%)[4,5]. Therefore, we recommend that medium-risk patients be managed according to standard preventive strategies outlined in existing guidelines, including the use of nonselective beta-blockers (*e.g.*, propranolol) to reduce portal pressure and regular endoscopic surveillance to monitor variceal progression. For patients with high-risk features of variceal bleeding (*e.g.*, severe varices or red wale marks) or significantly elevated portal pressure (hepatic venous pressure gradient > 12 mmHg), enhanced endoscopic therapy and medication management are recommended to further reduce bleeding risk, along with close monitoring of disease progression. If conventional treatment is ineffective or the condition continues to worsen, early TIPS intervention should be considered to further reduce the risk of bleeding[7].

For low-risk patients, the incidence of variceal bleeding was only 2.2%, indicating a low overall bleeding risk. For these patients, we recommend regular follow-up and monitoring of hepatic venous outflow patency, with timely adjustment of management strategies if significant changes in imaging parameters or hemodynamic indicators are observed[38]. The use of nonselective beta-blockers (*e.g.*, propranolol) in low-risk patients should be approached cautiously, especially in cases of hemodynamic instability or poor liver function reserve, where a thorough evaluation of potential adverse effects and benefits is necessary to avoid unnecessary interventions and treatments[39].

This study developed and validated a noninvasive risk prediction model integrating radiomics and clinical characteristics, demonstrating excellent predictive performance and clinical utility. However, several limitations need to be addressed. First, as a retrospective study, potential selection bias and the limited sample size may affect the generalization of the findings. While BCS in western populations is often driven by thrombophilic states (*e.g.*, factor V Leiden mutation), BCS in China predominantly arises from membranous obstruction of the inferior vena cava or short-segment hepatic vein stenosis. Consequently, our institutional protocol favors endovascular interventions (*e.g.*, angioplasty or TIPS), followed by bridging low-molecular-weight heparin and long-term warfarin therapy, rather than routine thrombophilia workup or first-line use of direct oral anticoagulants[2]. Therefore, larger multicenter or prospective studies - including settings where thrombophilia-driven BCS prevails - are needed to validate the stability and applicability of our model across diverse etiological and therapeutic contexts. Second, the use of single-level ROIs for the liver and spleen may not fully capture the heterogeneity of the entire organ. Although these specific levels are clinically relevant for assessing portal and splenic hemodynamics, volumetric ROIs or multislice approaches should be considered to better characterize tissue variability. Finally, greater automation and standardization of radiomics feature extraction would enhance the clinical feasibility of the model. Global validation in broader populations remains critical to confirm the robustness and facilitate wider adoption of this approach.

CONCLUSION

This study was the first to combine radiomics and clinical characteristics to develop a noninvasive model capable of predicting variceal bleeding risk in BCS patients with GEVs. The model demonstrated excellent predictive performance in clinical applications and provides robust support for individualized patient management and treatment strategies.

ACKNOWLEDGMENTS

We would like to thank our colleagues in the Department of Hepatopancreatobiliary Surgery and the Department of Hematology at Zhengzhou University People's Hospital, as well as those in the Department of Hepatopancreatobiliary Surgery at The First Affiliated Hospital of Zhengzhou University for their valuable contributions.

FOOTNOTES

Author contributions: Wang ZD and Nan HJ contributed equally to this work as co-first authors; they were responsible for designing the study, collecting and analyzing data, and writing the manuscript; Dang XW and Bai YL contributed equally by guiding the overall content and ensuring the scientific rigor of the article as co-corresponding authors; Dang XW is designated as the primary corresponding author for journal communications; Li SX, Li LH, Liu ZC, Guo HH, Li L, Liu SY and Li H provided technical support; all authors have read and approve the final manuscript.

Supported by Natural Science Foundation of Henan Province, China, No. 232300420232; and Henan Provincial Key Research and Development Project, No. 231111313500.

Institutional review board statement: The study was reviewed and approved by the Ethics Committee of the First Affiliated Hospital of Zhengzhou University (No. 2021-KY-1137-002).

Informed consent statement: As a retrospective observational study, the requirement for informed consent was waived. To ensure confidentiality, all private patient information was deidentified before analysis.

Conflict-of-interest statement: The authors declare that the research was conducted in the absence of any commercial or financial relationships.

Data sharing statement: The data supporting the findings of this study are included in the article and its supplementary materials. Further inquiries can be directed to the corresponding authors.

Country of origin: China

ORCID number: Lu-Hao Li 0000-0001-6676-3914; Yan-Liang Bai 0000-0003-2422-7720; Xiao-Wei Dang 0000-0001-7940-6385.

S-Editor: Lin C
L-Editor: A
P-Editor: Zhao S

REFERENCES

1 **Borsani O**, Pietra D, Rumi E. Primary Budd-Chiari Syndrome. *N Engl J Med* 2023; **389**: 769 [PMID: 37611130 DOI: 10.1056/NEJMc2305391]

2 **Budd-Chiari Syndrome and Hepatic Vascular Diseases Professional Committee of Chinese Research Hospital Association**. [Chinese multidisciplinary collaborative expert consensus for the diagnosis and treatment of Budd-Chiari syndrome (2021 version)]. *Zhonghua Wai Ke Za Zhi* 2022; **60**: 329-336 [PMID: 35272423 DOI: 10.3760/cma.j.cn112139-20211224-00619]

3 **Shukla A**, Shreshtha A, Mukund A, Bihari C, Eapen CE, Han G, Deshmukh H, Cua IHY, Lesmana CRA, Al Meshtab M, Kage M, Chaiteeraki R, Treeprasertsuk S, Giri S, Punamiya S, Paradis V, Qi X, Sugawara Y, Abbas Z, Sarin SK. Budd-Chiari syndrome: consensus guidance of the Asian Pacific Association for the study of the liver (APASL). *Hepatol Int* 2021; **15**: 531-567 [PMID: 34240318 DOI: 10.1007/s12072-021-10189-4]

4 **Zhang Q**, Niu S, Yang L, Zhu B, Shi K, Zhang X, Zhang Y, Bi Y, Mu Y, Wang X. A novel prognostic model for predicting the risk of first variceal hemorrhage in patients with HBV-related cirrhosis. *Front Cell Infect Microbiol* 2023; **13**: 1062172 [PMID: 36733609 DOI: 10.3389/fcimb.2023.1062172]

5 **Chen J**, Luo S, Tang F, Han M, Zheng J, Deng M, Luo G. Development and validation of a practical prognostic nomogram for evaluating

inpatient mortality of cirrhotic patients with acute variceal hemorrhage. *Ann Hepatol* 2023; **28**: 101086 [PMID: 36889674 DOI: 10.1016/j.aohep.2023.101086]

6 **Zhou PL**, Wu G, Han XW, Yan L, Zhang WG. Budd-Chiari syndrome with upper gastrointestinal hemorrhage: Characteristic and long-term outcomes of endovascular treatment. *Vascular* 2017; **25**: 642-648 [PMID: 28610476 DOI: 10.1177/1708538117710087]

7 **Gralnek IM**, Camus Duboc M, Garcia-Pagan JC, Fuccio L, Karstensen JG, Hucl T, Jovanovic I, Awadie H, Hernandez-Gea V, Tantau M, Ebigbo A, Ibrahim M, Vlachogiannakos J, Burgmans MC, Rosasco R, Triantafyllou K. Endoscopic diagnosis and management of esophagogastric variceal hemorrhage: European Society of Gastrointestinal Endoscopy (ESGE) Guideline. *Endoscopy* 2022; **54**: 1094-1120 [PMID: 36174643 DOI: 10.1055/a-1939-4887]

8 **Whybra P**, Zwanenburg A, Andrearczyk V, Schaer R, Apte AP, Ayotte A, Baheti B, Bakas S, Bettinelli A, Boellaard R, Boldrini L, Buvat I, Cook GJR, Dietsche F, Dinapoli N, Gabryś HS, Goh V, Guckenberger M, Hatt M, Hosseinzadeh M, Iyer A, Lenkowicz J, Loutfi MAL, Löck S, Marturano F, Morin O, Nioche C, Orlhac F, Pati S, Rahmim A, Rezaeijo SM, Rookyard CG, Salmanpour MR, Schindele A, Shiri I, Spezi E, Tanadini-Lang S, Tixier F, Upadhaya T, Valentini V, van Griethuysen JJM, Yousefirizi F, Zaidi H, Müller H, Vallières M, Depeursinge A. The Image Biomarker Standardization Initiative: Standardized Convolutional Filters for Reproducible Radiomics and Enhanced Clinical Insights. *Radiology* 2024; **310**: e231319 [PMID: 38319168 DOI: 10.1148/radiol.231319]

9 **Zwanenburg A**, Vallières M, Abdalah MA, Aerts HJWL, Andrearczyk V, Apte A, Ashrafinia S, Bakas S, Beukinga RJ, Boellaard R, Bogowicz M, Boldrini L, Buvat I, Cook GJR, Davatzikos C, Depeursinge A, Desseroit MC, Dinapoli N, Dinh CV, Echegaray S, El Naqa I, Fedorov AY, Gatta R, Gillies RJ, Goh V, Götz M, Guckenberger M, Ha SM, Hatt M, Isensee F, Lambin P, Leger S, Leijenaar RTH, Lenkowicz J, Lippert F, Losnegård A, Maier-Hein KH, Morin O, Müller H, Napel S, Nioche C, Orlhac F, Pati S, Pfaehler EAG, Rahmim A, Rao AUK, Scherer J, Siddique MM, Sijtsema NM, Socarras Fernandez J, Spezi E, Steenbakkers RJHM, Tanadini-Lang S, Thorwarth D, Troost EGC, Upadhaya T, Valentini V, van Dijk LV, van Griethuysen J, van Velden FHP, Whybra P, Richter C, Löck S. The Image Biomarker Standardization Initiative: Standardized Quantitative Radiomics for High-Throughput Image-based Phenotyping. *Radiology* 2020; **295**: 328-338 [PMID: 32154773 DOI: 10.1148/radiol.2020191145]

10 **Guiot J**, Vaidyanathan A, Deprez L, Zerka F, Danthine D, Frix AN, Lambin P, Bottari F, Tsoutzidis N, Miraglio B, Walsh S, Vos W, Hustinx R, Ferreira M, Lovinfosse P, Leijenaar RTH. A review in radiomics: Making personalized medicine a reality *via* routine imaging. *Med Res Rev* 2022; **42**: 426-440 [PMID: 34309893 DOI: 10.1002/med.21846]

11 **Mayerhoefer ME**, Materka A, Langs G, Häggström I, Szczypiński P, Gibbs P, Cook G. Introduction to Radiomics. *J Nucl Med* 2020; **61**: 488-495 [PMID: 32060219 DOI: 10.2967/jnumed.118.222893]

12 **Bera K**, Braman N, Gupta A, Velcheti V, Madabhushi A. Predicting cancer outcomes with radiomics and artificial intelligence in radiology. *Nat Rev Clin Oncol* 2022; **19**: 132-146 [PMID: 34663898 DOI: 10.1038/s41571-021-00560-7]

13 **Harding-Theobald E**, Louissaint J, Maraj B, Cuaresma E, Townsend W, Mendiratta-Lala M, Singal AG, Su GL, Lok AS, Parikh ND. Systematic review: radiomics for the diagnosis and prognosis of hepatocellular carcinoma. *Aliment Pharmacol Ther* 2021; **54**: 890-901 [PMID: 34390014 DOI: 10.1111/apt.16563]

14 **Liu Z**, Wang S, Dong D, Wei J, Fang C, Zhou X, Sun K, Li L, Li B, Wang M, Tian J. The Applications of Radiomics in Precision Diagnosis and Treatment of Oncology: Opportunities and Challenges. *Theranostics* 2019; **9**: 1303-1322 [PMID: 30867832 DOI: 10.7150/thno.30309]

15 **Luo R**, Gao J, Gan W, Xie WB. Clinical-radiomics nomogram for predicting esophagogastric variceal bleeding risk noninvasively in patients with cirrhosis. *World J Gastroenterol* 2023; **29**: 1076-1089 [PMID: 36844133 DOI: 10.3748/wjg.v29.i6.1076]

16 **Yang JQ**, Zeng R, Cao JM, Wu CQ, Chen TW, Li R, Zhang XM, Ou J, Li HJ, Mu QW. Predicting gastro-oesophageal variceal bleeding in hepatitis B-related cirrhosis by CT radiomics signature. *Clin Radiol* 2019; **74**: 976.e1-976.e9 [PMID: 31604574 DOI: 10.1016/j.crad.2019.08.028]

17 **Lin Y**, Li L, Yu D, Liu Z, Zhang S, Wang Q, Li Y, Cheng B, Qiao J, Gao Y. A novel radiomics-platelet nomogram for the prediction of gastroesophageal varices needing treatment in cirrhotic patients. *Hepatol Int* 2021; **15**: 995-1005 [PMID: 34115257 DOI: 10.1007/s12072-021-10208-4]

18 **Meng D**, Wei Y, Feng X, Kang B, Wang X, Qi J, Zhao X, Zhu Q. CT-Based Radiomics Score Can Accurately Predict Esophageal Variceal Rebleeding in Cirrhotic Patients. *Front Med (Lausanne)* 2021; **8**: 745931 [PMID: 34805214 DOI: 10.3389/fmed.2021.745931]

19 **Turon F**, Casu S, Hernández-Gea V, Garcia-Pagán JC. Variceal and other portal hypertension related bleeding. *Best Pract Res Clin Gastroenterol* 2013; **27**: 649-664 [PMID: 24160925 DOI: 10.1016/j.bpg.2013.08.004]

20 **Diaz-Soto MP**, Garcia-Tsao G. Management of varices and variceal hemorrhage in liver cirrhosis: a recent update. *Therap Adv Gastroenterol* 2022; **15**: 17562848221101712 [PMID: 35757384 DOI: 10.1177/17562848221101712]

21 **Wang Z**, Wang Z, Zhang Z, Li J, Pan Z, Liu A, Lu J, Guo J, Zu M, Xu H. Establishment and validation of a prediction model for the first recurrence of Budd-Chiari syndrome after endovascular treatment: a large sample size, single-center retrospective study. *Hepatol Int* 2023; **17**: 159-169 [PMID: 36567373 DOI: 10.1007/s12072-022-10464-y]

22 **Cheng D**, Xu H, Lu ZJ, Hua R, Qiu H, Du H, Xu X, Zhang J. Clinical features and etiology of Budd-Chiari syndrome in Chinese patients: a single-center study. *J Gastroenterol Hepatol* 2013; **28**: 1061-1067 [PMID: 23425079 DOI: 10.1111/jgh.12140]

23 **Rautou PE**, Douarin L, Denninger MH, Escolano S, Lebrec D, Moreau R, Vidaud M, Itzykson R, Moucari R, Bezeaud A, Valla D, Plessier A. Bleeding in patients with Budd-Chiari syndrome. *J Hepatol* 2011; **54**: 56-63 [PMID: 20889223 DOI: 10.1016/j.jhep.2010.06.019]

24 **Sharma A**, Goel A, Moses V, Keshava SN, Zachariah UG, Elias E, Eapen CE. Anticoagulating Budd-Chiari syndrome patients presenting with variceal bleed: A retrospective study. *J Gastroenterol Hepatol* 2020; **35**: 1397-1403 [PMID: 31900982 DOI: 10.1111/jgh.14971]

25 **Bizzaro D**, Becchetti C, Trapani S, Lavezzo B, Zanetto A, D'Arcangelo F, Merli M, Lapenna L, Invernizzi F, Taliani G, Burra P; AISF Special Interest Group on Gender in Hepatology. Influence of sex in alcohol-related liver disease: Pre-clinical and clinical settings. *United European Gastroenterol J* 2023; **11**: 218-227 [PMID: 36866682 DOI: 10.1002/ueg2.12370]

26 **Neong SF**, Billington EO, Congly SE. Sexual Dysfunction and Sex Hormone Abnormalities in Patients With Cirrhosis: Review of Pathogenesis and Management. *Hepatology* 2019; **69**: 2683-2695 [PMID: 30468515 DOI: 10.1002/hep.30359]

27 **Rauch U**. Gender differences in anticoagulation and antithrombotic therapy. *Handb Exp Pharmacol* 2012; 523-542 [PMID: 23027465 DOI: 10.1007/978-3-642-30726-3_23]

28 **Mendizabal M**, Cançado GGL, Albillos A. Evolving portal hypertension through Baveno VII recommendations. *Ann Hepatol* 2024; **29**: 101180 [PMID: 37984701 DOI: 10.1016/j.aohep.2023.101180]

29 **Brusilovskaya K**, Hofer BS, Simbrunner B, Eichelberger B, Lee S, Bauer DJM, Mandorfer M, Schwabl P, Panzer S, Reiberger T, Gremmel T. Platelet Function Decreases with Increasing Severity of Liver Cirrhosis and Portal Hypertension-A Prospective Study. *Thromb Haemost* 2023; **123**: 1140-1150 [PMID: 37517407 DOI: 10.1055/s-0043-1771187]

30 **Darwish Murad S**, Plessier A, Hernandez-Guerra M, Fabris F, Eapen CE, Bahr MJ, Trebicka J, Morard I, Lasser L, Heller J, Hadengue A, Langlet P, Miranda H, Primignani M, Elias E, Leebeek FW, Rosendaal FR, Garcia-Pagan JC, Valla DC, Janssen HL; EN-Vie (European Network for Vascular Disorders of the Liver). Etiology, management, and outcome of the Budd-Chiari syndrome. *Ann Intern Med* 2009; **151**: 167-175 [PMID: 19652186 DOI: 10.7326/0003-4819-151-3-200908040-00004]

31 **Porrello G**, Mamone G, Miraglia R. Budd-Chiari Syndrome Imaging Diagnosis: State of the Art and Future Perspectives. *Diagnostics (Basel)* 2023; **13** [PMID: 37443650 DOI: 10.3390/diagnostics13132256]

32 **Kim SH**, Kim YJ, Lee JM, Choi KD, Chung YJ, Han JK, Lee JY, Lee MW, Han CJ, Choi JI, Shin KS, Choi BI. Esophageal varices in patients with cirrhosis: multidetector CT esophagography--comparison with endoscopy. *Radiology* 2007; **242**: 759-768 [PMID: 17229872 DOI: 10.1148/radiol.2423050784]

33 **Salahshour F**, Mehrabinejad MM, Rashidi Shahpasandi MH, Salahshour M, Shahsavari N, Nassiri Toosi M, Ayoobi Yazdi N. Esophageal variceal hemorrhage: the role of MDCT characteristics in predicting the presence of varices and bleeding risk. *Abdom Radiol (NY)* 2020; **45**: 2305-2314 [PMID: 32447415 DOI: 10.1007/s00261-020-02585-5]

34 **Calame P**, Ronot M, Bouveresse S, Cervoni JP, Vilgrain V, Delabrousse É. Predictive value of CT for first esophageal variceal bleeding in patients with cirrhosis: Value of para-umbilical vein patency. *Eur J Radiol* 2017; **87**: 45-52 [PMID: 28065374 DOI: 10.1016/j.ejrad.2016.12.006]

35 **Vashishtha C**, Sarin SK. Bleeding Complications of Portal Hypertension. *Clin Liver Dis* 2024; **28**: 483-501 [PMID: 38945639 DOI: 10.1016/j.cld.2024.03.006]

36 **Inchingolo R**, Posa A, Mariappan M, Tibana TK, Nunes TF, Spiliopoulos S, Brountzos E. Transjugular intrahepatic portosystemic shunt for Budd-Chiari syndrome: A comprehensive review. *World J Gastroenterol* 2020; **26**: 5060-5073 [PMID: 32982109 DOI: 10.3748/wjg.v26.i34.5060]

37 **Vizzutti F**, Schepis F, Arena U, Fanelli F, Gitto S, Aspite S, Turco L, Dragoni G, Laffi G, Marra F. Transjugular intrahepatic portosystemic shunt (TIPS): current indications and strategies to improve the outcomes. *Intern Emerg Med* 2020; **15**: 37-48 [PMID: 31919780 DOI: 10.1007/s11739-019-02252-8]

38 **Kaplan DE**, Ripoll C, Thiele M, Fortune BE, Simonetto DA, Garcia-Tsao G, Bosch J. AASLD Practice Guidance on risk stratification and management of portal hypertension and varices in cirrhosis. *Hepatology* 2024; **79**: 1180-1211 [PMID: 37870298 DOI: 10.1097/HEP.0000000000000647]

39 **Turco L**, Reiberger T, Vitale G, La Mura V. Carvedilol as the new non-selective beta-blocker of choice in patients with cirrhosis and portal hypertension. *Liver Int* 2023; **43**: 1183-1194 [PMID: 36897563 DOI: 10.1111/liv.15559]

Published by **Baishideng Publishing Group Inc**
7041 Koll Center Parkway, Suite 160, Pleasanton, CA 94566, USA
Telephone: +1-925-3991568
E-mail: office@baishideng.com
Help Desk: https://www.f6publishing.com/helpdesk
https://www.wjgnet.com